Iranian Journal of Analytical Chemistry **مجله ایرانی شیمی تجزیه**
Volume 8, Issue 2, September 2021 (40-49) Origonal Research Article دوره۸، شماره ۲، مهرماه ۱۴۰۰ (۴۹-۴۰)

Study on Electrochemical Behavior of Hydrazine at a Glassy Carbon Electrode Modified with Polymer Thin Films Embedded Copper Nanoparticles

Ghasem Karim-Nezhad[*1], **Sara Pashazadeh**[2], **Samira Honarmand**[1]
1. Department of Chemistry, Payame Noor University, PO BOX 19395-3697, Tehran, Iran
2. Electroanalytical Chemistry Laboratory, Department of Chemistry, Faculty of Sciences, Azarbaijan Shahid Madani University, Tabriz 53714-161, Iran

Received: 26 July 2021 **Accepted:** 9 September 2021
DOI: 10.30473/ijac.2022.62498.1214

Abstract
In this study, a novel and convenient electrochemical sensor was fabricated by using dripping well-dispersed graphene oxide nanosheets, electropolymerization of poly glycine (p-Gly) and in situ plating of metallic copper nanoparticle film methods, successively. This sensor was further employed to investigate the electrochemical behavior of hydrazine. Scanning electron microscopy and energy dispersive X-ray spectrometry were used for the characterization of the prepared film. Anodic peak potential of hydrazine oxidation at the surface of modified electrode shifts by about 150 mV toward negative values compared with that on the bare electrode. The kinetic parameters such as the electron transfer coefficient (*α*) and charge transfer rate constant (*k*) for the oxidation of hydrazine was determined utilizing cyclic voltammetry (CV). The diffusion coefficient (*D*) of hydrazine was also estimated using chronoamperometry. The dynamic detection range of this sensor to hydrazine was 5- 60 and 80-150 µM at the modified electrode surface using an amperometric method. The detection limit and quantitation are 5.33 µM and 17.77 µM, respectively. A new voltammetric method for determination of hydrazine was erected and shows good sensitivity and selectivity, wider linear relationship, very easy surface update and good stability.

Keywords
Hydrazine; Modified Glassy Carbon Electrode; Copper Nanoparticle; Glycine. Graphene Oxide Nanosheets .

1. INTRODUCTION

Graphene and related materials such as graphene oxide, reduced graphene oxide, etc have grabbed great attention since its successful isolation in 2004 [1]. Graphene (Gr) is a two dimensional (2D) one atom thick nanomaterial consisting of sp^2 hybridized carbon, has attracted tremendous attention due to its unique properties, such as excellent electronic conductivity, large specific surface area, strong mechanical strength, and enhanced electrocatalytic activity [1, 2] Graphene has been obtained so far by several techniques : mechanical cleavage of graphite [3], epitaxial growth on single-crystal silicon carbide as well as metals [4], thermal expansion of graphite [5], and chemical reduction of graphene oxide (GO) [6,7]. It is reported that compared to single-walled carbon nanotubes, graphene exhibits 60 times more conductivity, better sensitivity and stability, greater sp^2 character, and also more surface negative charge density[8, 9]. Due to its outstanding physicochemical properties, graphene has been used for a wide range of applications including electrochemical sensors, supercapacitors, batteries, electronics, fuel cells, and biosensors [10]. One of the promising applications of graphene is the construction of chemical modified electrodes in the area of sensors, owing to its merits of large surface area, excellent conductivity, strong mechanical strength, and unique electronic properties [11–13]. It has been employed as modification materials on the surface of glassy carbon electrodes (GCE) and carbon fiber electrodes serving as an electrochemical sensor.

Recently, the nanocomposites of metal nanoparticles (MNPs) with GO have attracted much interest in the construction of electrochemical sensors due to their synergistic and novel properties. The GO combined with metallic composite materials can improve the hybrid's electronic and thermal conductivity [14]. Metallic nanoparticles have found utility in catalytic applications. Since the surface area of a catalyst is a critical factor, metallic nanoparticles, having an immense surface area compared to conventional materials, have been intensely investigated [15]. Among the various nanostructured materials, copper nanoparticles (Cu-NPs) in particular have received significant interest, due to their excellent electrocatalytic ability that has been widely employed in various potential disciplines including electrochemical sensors and biosensors [16] due to their low cost, high specific surface area, good electrocatalytic

---

*Corresponding Author: g.knezhad@gmail.com activity, and the possibility of promoting electron transfer reactions at a lower overpotential [17].

Polymer modified electrodes have been paid increasing attention in the electrochemical analysis due to their more active sites, excellent perm selectivity, good stability, and strong adherence to electrode surface [18]. Electropolymerization, among deposition methods, is a nice approach to immobilize polymers to produce a proper substrate for MNPs. By adjusting the electrochemical parameters, the film thickness, permeability, and charge transfer characteristics can be controlled. Several modified electrodes have been reported that conductive polymers, such as polypyrrole [19], polyaniline [20, 21], poly- arginine [22], or poly-glutamic acid [23], have been directly deposited on electrode surfaces by electropolymerization.

We are interested here in applying graphene oxide nanosheets as the support (electrode material) for the electrochemical oxidation of hydrazine. Hydrazine is widely used in rocket fuels, fuel cells, pesticides, photography chemicals, weapons for mass destruction, and so on [24,25]. Also, hydrazine is very important in pharmacology because it has been recognized as a carcinogenic and hepatotoxic substance, which affects the liver and brain glutathione. Consequently, drug regulatory authorities are becoming increasingly aware of the need to control the levels of hydrazones in isoniazid and other hydrazide drugs and their formulations. Despite the wide use of hydrazine in various areas, it has been known to be harmful to human life. Therefore, a highly sensitive method is necessary for the reliable measurement of hydrazine concentration and the electrooxidation of hydrazine is a reaction of practical importance.

Herein, we developed copper nanoparticles/poly (glycine)/ graphene oxide nanosheets modified glassy carbon electrode (Cu-NPs/P-Gly/GONs/GCE) as an efficient and stable electrochemical sensor for hydrazine detection. By combining the benefits of Cu nanoparticles and polyglycine/ graphene oxide nanosheets, this prepared modified GCE exhibited excellent electrocatalytic activity to the oxidation of hydrazine.

2. EXPERIMENTAL

2.1. Chemicals and reagents

All solvents and reagents were purchased from Aldrich or Merck and were used without further purification. All solutions were prepared with double-distilled water.

2.2. Apparatus

Electrochemical experiments were performed using an AUTOLAB modular electrochemical system (Eco Chem. Utrecht, The Netherlands) equipped with a PGSTAT-12 model and driven by GPES 4.9 software. A conventional three-electrode cell was used with an Ag/AgCl/KCl (3 M) as a reference electrode, a Pt wire as the counter electrode, and a modified glassy carbon electrode (GCE) as the working electrode.

pH measurements were performed using a Jenway 3345 Model pH meter equipped with a combined glass electrode. The surface morphology and properties of the modified electrode were characterized by field emission scanning electron microscopy (FESEM Vega-Tescan).

2.3. Synthesis of graphene oxide nanosheets

GO was prepared from natural graphite by using a modified Hummers 'method [26]. In a typical preparation ,10g of graphite was added into 230 mL of cooled sulphuric acid) placed in an ice bath). Then, 30 g of $KMnO_4$ and 5 g of $NaNO_3$ were added gradually with stirring and cooling so that the temperature of the mixture was maintained at 10–15 °C. The mixture was then heated and stirred at 35 °C for 30 min. The temperature was raised to 90 °C after 250 mL of doubly distilled water was slowly added. The mixture was stirred at 90 °C for 30 min. To stop the oxidation reaction ,an additional 500 mL of deionized water and 50 mL of 30% hydrogen peroxide solution (H_2O_2), were added sequentially to reduce the excess $KMnO_4$. The obtained sample was filtered and washed with 100 mL of deionized water. The filtrate was resuspended in deionized water again ,and followed by ultrasonic treatment for15 min. The solid product was separated by centrifugation and then dried in a vacuum oven at 60 °C for 24 h.

2.4. Construction of Cu-NPs/p-Gly/GONs/GCE

The procedure of preparation of the working electrode was as follows: first, GCE was carefully polished mechanically with Al_2O_3 slurry (0.05 µm) on the polishing cloth and then rinsed with double distilled water. In order to prepare GONs/GCE, a solution of GONs in doubly distilled water (5 µl of 1 mg/mL) under ultrasonic radiation was drop-coated onto the GCE surface and dried at room temperature. GONs/GCE was immersed in a 10 mM glycine aqueous solution (pH 7.0), and cyclic voltammetry was carried out in the potential range of -0.5 and 1.8 V at a scan rate of 100 mV s^{-1} (10 cycles). In this step, poly- glycine (p-Gly) was deposited on the electrode. The obtained modified electrode (p-Gly /GONs/GCE) was washed with water and dried in air. Finally, metallic Cu-nanoparticles (Cu-NPs) were electrochemically deposited by cycling the potential from 0.0 to +1.1 V in $CuSO_4$ (20 mM in H_2SO_4 solution) at a scan rate of 50 mV s^{-1} (17 cycles). The obtained modified electrode (Cu-NPs/p-Gly/GONs/GCE) was washed with ultrapure water several times. Stepwise electrodes were also prepared with the same procedures described above, for comparison purposes.

3. RESULT AND DISCUSSION

3.1. Characterization of the modified electrode

The typical morphologies of the bare GCE (Fig. 1A), GONs/GCE (Fig. 1B) and Cu-NPs/p-Gly/GONs/GCE (Fig. 1C) were characterized by field emission scanning electron microscopy (FESEM).

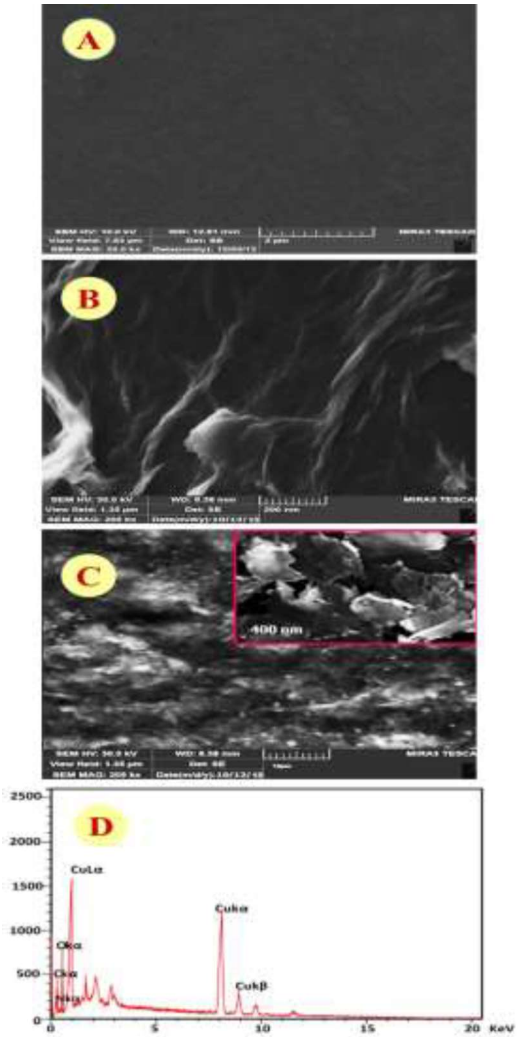

Fig. 1. Field emission scanning electron micrographs (FESEM) of GCE (A), GONs/GCE (B), and CuNPs/P-Gly/GONs/GCE (C). Energy-dispersive X-ray spectrum (EDS) of CuNPs/P-Gly/GONs/GCE (D).

As expected, GONs layer on GCE produces crude and folded surface (B). The whole assembly on the electrode surface (Cu-NPs/p-Gly/GONs/GCE) is shown in image C. The surface morphology was changed and gave clear evidence for the successful fabrication of Cu-NPs/p-Gly/GONs/GCE on the surface of GCE. From Fig. 1C it was evident that Cu-NPs with 90 nm average diameter were homogeneously distributed throughout the film. Energy Dispersive X-ray spectrum (EDS) of Cu-NPs/p-Gly/GONs film showed specific regions of copper atoms and confirmed the deposition of Cu particles on the modified electrode (Fig. 1D).

3.2. Electrochemical behaviors of hydrazine on Cu-NPs/p-Gly/GONs/GCE

The electrochemical behaviors of hydrazine at seven different working electrodes (unmodified GCE, GONs/GCE, Cu-NP/GCE, P-Gly/GCE, P-Gly/GONs/GCE, Cu-NP/GONs/GCE, and Cu-NPs/p-Gly/GONs/GCE) in phosphate buffer of pH 7.0 were compared by cyclic voltammetry, and the results are shown in Fig. 2. At unmodified GCE, hydrazine showed a broad anodic peak at 665 mV with a very low current response. Electrochemical responds of hydrazine at the bare GCE indicated slow electron transfer. An anodic current peak of hydrazine at 656, 645 and 605 mV was obtained at GONs/GCE, P-Gly/GCE, P-Gly/GONs/GCE. The peak current hydrazine was enhanced compared to that at bare GCE. These findings indicated good conductive performance of GONs and excellent catalytic ability of P-Gly film on hydrazine. The highest improvement of the anodic peak current and good negative shift anodic peak potential of hydrazine was obtained, when Cu-NPs doped in polymeric film at the Cu-NPs/p-Gly/GONs/GCE /GCE (curves g).

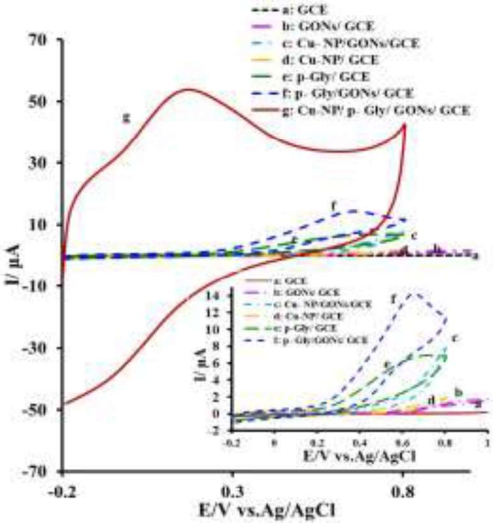

Fig. 2. Cyclic voltammograms of 150 µM hydrazine in 0.1 M PBS (pH 7.0) at unmodified GCE (a) GONs/GCE (b) P-Gly/GCE (c) CuNPs/GCE (d) CuNPs/GONs/GCE (e) P-Gly/GONs/GCE(f) and CuNPs/P-Gly/GONs/GCE (g) at 50 mV s^{-1}.

3.3. The effect of pH

One parameter affecting the electrochemical response of the Cu-NPs/p-Gly/GONs/GCE is the pH of the supporting electrolyte. The oxidation of hydrazine shows a strong dependence on pH. In general, since hydrazine contains NH_2 groups, it was anticipated that the electrochemical behavior of the compound would be pH-dependent. The effect of pH on the electrochemical behavior of hydrazine on the surface of the Cu-NPs/p-Gly/GONs/GCE electrode is shown in Fig. 3.

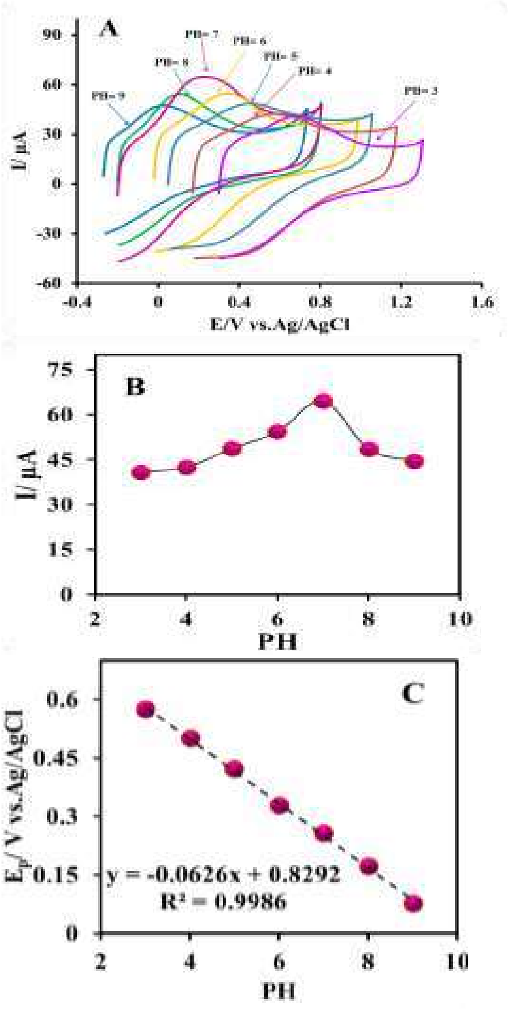

Fig. 3. Cyclic voltammograms of 200 µM hydrazine on CuNPs/P-Gly/GONs/GCE in various pHs (3.0, 4.0, 5.0, 6.0, 7.0, 8.0 and 9.0) of supporting electrolyte solution, (B) variation of the oxidation peak current (i_p) with pH solution (C) variation of the oxidation peak potential (E_p) with pH solution; scan rate: 50 mVs^{-1}.

The anodic peak currents of hydrazine increased with increasing pH from 2.0 to 6.0. The maximum current response, as well as a break in potential curve for oxidation of hydrazine, is achieved at a neutral pH value (pH 7. 0) as shown in Fig. 3. Therefore, a 0.1 M phosphate buffer solution (PBS) with pH 7.0 was selected. In addition, all anodic peak currents for oxidation of hydrazine shifted towards more negative potential with an increase in pH, showing that protons have taken part in their electrode reaction processes. Linear relationships of the peak potential of hydrazine and the pH were E_{pa}=0.8292 - 0.0626 pH, R^2 = 0.9986 with the slope of 62.6 mV per pH (Fig. 3C). This result was close to the expected Nernstian theoretical value of 59.0 mV per pH unit suggested that equal numbers of electron and proton transferred were involved in the electrode reactions.

3.4. Effect of scan rate on the oxidation of hydrazine

Electrochemical mechanisms usually can be acquired from the relationship between peak current and scan rate. The influence of scan rate was investigated in the range of 5-170 mV s^{-1} on the electrochemical behavior of Cu-NPs/p-Gly/GONs/GCE in the presence of hydrazine. Peak currents of the Cu-NPs/p-Gly/GONs/GCE increased with the increment of the scan rate. A good linear relationship could be observed between the peak current and square root of scan rate in the range of 5–170 mV s^{-1} (Fig. 4A). For 200 µM of hydrazine, the anodic peak followed the linear regression equation I_{pa} (µA) = –8.378 + 11.43 $v^{1/2}$ ($mV^{1/2}$ $s^{-1/2}$) (R^2 = 0.9906), which indicates that the electrode process was controlled by diffusion of hydrazine to the electrode surface, rather than adsorption (Fig. 4B). In addition, there was a linear relation between log (I_P/µA) and log (v/mVs^{-1}), corresponding to the following equation: log (I_P/µA) = 0.6297 log (v/mVs^{-1}) + 0.7129; R^2=0.9949 (Fig. 4C). The slope of 0.6297 was very close to the theoretically expected value of 0.5 for diffusion-controlled processes.

For determination of the transfer coefficient (α) and the number of electrons involved in the rate-determining (n_α), the Tafel plot was drawn (not shown here) using the data from the rising part of the current-voltage curve at scan rate 10 mV s^{-1}. The Tafel slope was 150.7 mV $decade^{-1}$ and by considering that α equals 0.4, the results indeed suggest one-electron (n_α= 0.78≅ 1) transfer process in the rate-determining step for the electrocatalytic oxidation of hydrazine. The Tafel slope could be calculated by another method, i.e. it can be determined from the following equation [27]:

$$E_{\mathrm{P}} = \frac{b}{2}\log v + \mathrm{k} \qquad (1)$$

Where b is the Tafel slope and k is a constant value. Fig. 4D shows the plot of E_P versus log (v). The slope of this plot is 86.6 mV, therefore, the slope becomes 173 mV $decade^{-1}$.

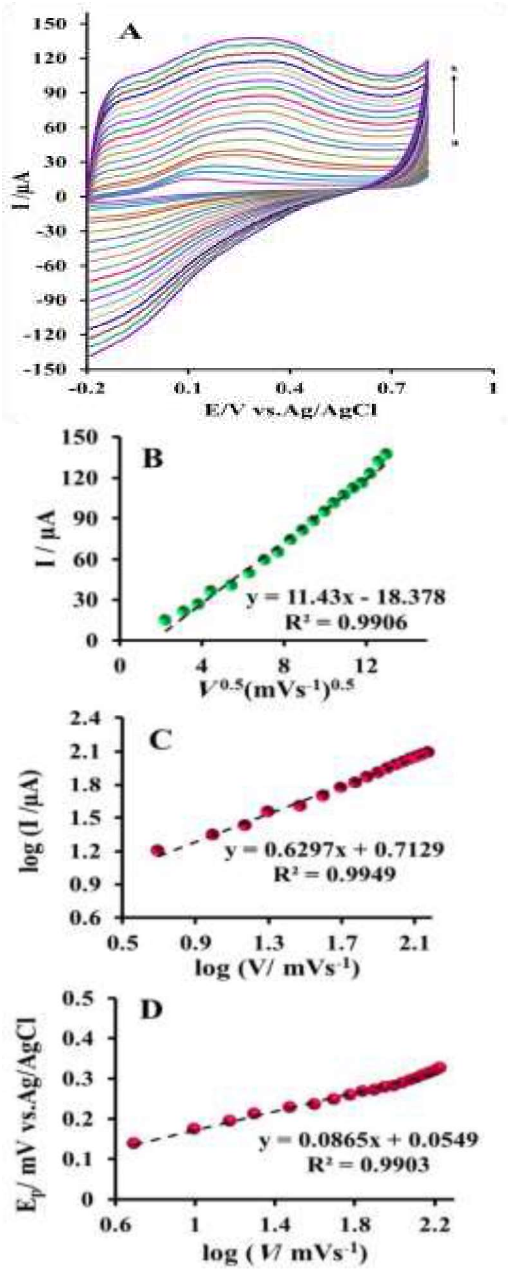

Fig. 4. (A) Effect of scan rate (5-170 mV s^{-1}) on the oxidation behavior of hydrazine in PBS (0.1 M, pH 7.0) at CuNPs/P-Gly/GONs/GCE; (B) Linear relationship of I_p against $v^{1/2}$; (C) log I against log v.(D) The plot of E_P vs. log v.

This result is close to that obtained from the rising part of the voltammogram recorded at the 10 mVs^{-1}. If α was assumed equal to 0.65, n_α is 1. A total number of electrons (n) in the oxidation process was calculated according to the following equation for an irreversible diffusive process [28]:

$$I_p = 3.01\times10^5 n[(1-\alpha)n_\alpha]^{1/2} A C D^{1/2} v^{1/2} \quad (2)$$

With considering $[(1-\alpha)\ n_\alpha] = 0.4$, $D = 4.08\times10^{-6}$ cm^{2}s^{-1} (see chronoamperometric studies) and A= 0.0314 cm^2, it is estimated that the total number of the electrons involved in the anodic oxidation of hydrazine is n= 4.1 ≅ 4. Based on the above results the following mechanism can be proposed for the oxidation of hydrazine.

$N_2H_4 + OH^- \rightarrow N_2H_3 + H_2O + e^-$ (slow) (1)

$N_2H_3 + 3OH^- \rightarrow N_2 + 3H_2O + 3e^-$ (fast) (2)

The rate-determining step is a single electron transfer followed by a three-electron process to give N_2 as a final product.

3.5. Calibration curve

Since amperometry under stirred conditions has a much higher current sensitivity than cyclic voltammetry, it was used to estimate the lower limit of detection. Fig.5 shows chronoamperograms which were recorded from rotating disk modified glassy carbon electrode (rotation speed 1500 rpm) under conditions where the potential of the modified electrode was kept at 0.266 V during the successive addition of varying concentrations of hydrazine. As shown in the figure a well-defined response was observed during the stepwise increasing of hydrazine concentration in the range of 5- 60 and 80- 150 µM. It was observed that the sensor responds so rapidly to the substrate, as about 96% of the steady-state current appears within 50 s. The limits of detection (LOD) and quantization (LOQ) of the procedure were calculated according to the 3 SD/m and 10 SD/m criteria where SD is the standard deviation of the blank and m is the slope of the calibration curves [29]. The limits of detection and quantitation were found to be 5.33 µM and 17.77 µM for peak hydrazine. Table 1 lists the response characteristics of the proposed hydrazine sensor in comparison to other reported hydrazine sensors in the literature. As a show, the linear range and LOD of the proposed method are significantly compared with previous reports.

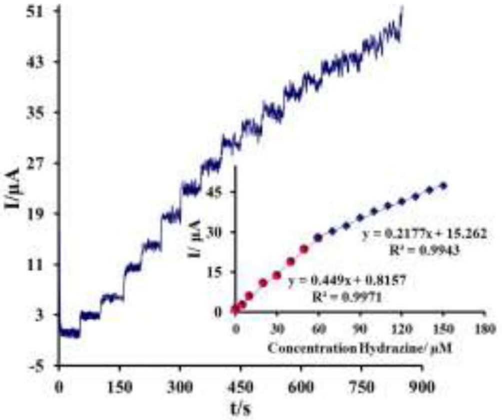

Fig. 5. Amperometric responses of the CuNPs/P-Gly/GONs/GCE to successive additions of hydrazine in 0.1 M PBS solution (pH=7.0) at 0.266 V *Insets*: plot of amperometric response versus the concentration of hydrazine from 5 to 60 and 60-150 µM.

Table 1. Comparison of analytical characteristics of CuNPs/P-Gly/GONs/GCE for the determination of hydrazine with other electrodes.

Electrode	Method	Linear range (μM)	Detection limit (μM)	Ref.
Copper (hydr)oxide/MCE	chronoamperometry	100-1800	-	[31]
Cobalt phthalocyanine/ MCPE	CV	125-980	73.5	[32]
Overoxidized polypyrrole/ GCE	amperometry	13-2000	3.6	[33]
NiHCF/CC	CV	20-2000	8	[34]
OMWCNT/GCE	DPV	0.6- 400	0.17	[35]
Pd/CNF–GCE	DPV	10-4000	2.9	[36]
Pd/BMWCNTs	LSV	56-157	10	[37]
Pyrogallol red/GCE	DPV	5-600	2	[38]
PdNPs–EDAC/GCE	DPV	5-150	1.5	[39]
Thiourea/ MCE	CV	130-5000	7.6	[40]
Gold nanoparticles/ titanium	CV	5000-40000	42	[41]
Ferrocene/ MCNPE	DPV	16-80	14	[42]
CuO/CNT/SPE	amperometry	5-50	5	[43]
Pt/ZnFe2O4/rGO/GCE	amperometry	0-1000	20	[44]
Chrysanthemum-like Co_3O_4/GCE	amperometry	50-1088	3.7	[45]
Cu-NP/p- Gly/GONs/GCE	amperometry	2-130	5.33	This work

3.6. Chronoamperometric Study

In order to evaluate the reaction kinetics, the oxidation of hydrazine on Cu-NPs/p-Gly/GONs/GCE was investigated by chronoamperometry.

Chronoamperometric measurements of hydrazine at Cu-NPs/p-Gly/GONs/GCE were carried out by setting the working electrode potential of 266 mV (at first potential step) and 0.0 mV (at second potential step) for various concentrations of hydrazine. The diffusion coefficient, *D*, of hydrazine in solution was determined using chronoamperometric studies. The chronoamperometric data of Fig. 6A present an obvious increasing trend of the current for the hydrazine oxidation with the addition of hydrazine concentrations. The experimental plots of I *vs* $t^{-1/2}$ with the best fits for different concentrations of hydrazine were shown in Fig. 6B. The slopes of the resulting straight lines were then plotted versus hydrazine concentrations (Fig. 6C). From whose slope, we calculated a diffusion coefficient ($D = 4.08\times10^{-6}$ cm^2 s^{-1}) for hydrazine using the Cottrell equation [27]. The rate constants of the reactions of hydrazine and the ensuing intermediates with the redox sites of the Cu-NPs/p-Gly/GONs/GCE electrode can be derived from the chronoamperograms according to Eq. (3) [30]:

$$I_{\text{catal}}/I_{\text{d}} = \lambda^{1/2}\left[\pi^{1/2}\,\text{erf}\left(\lambda^{1/2}\right) + \exp(-\lambda)\,/\,\lambda^{1/2}\right] \quad (3)$$

where I_{catal} is the catalytic current in the presence of hydrazine, I_d the limiting current in the absence of hydrazine and $\lambda = k\,Ct$ (*k, C* and t are the catalytic rate constant, the bulk concentration of hydrazine and the elapsed time, respectively) is the argument of the error function. For $\lambda > 1.5$, erf ($\lambda^{1/2}$) almost equals unity and Eq. (4) reduces to [30]:

$$I_{\text{catal}}/I_{\text{d}} = \lambda^{1/2}\pi^{1/2}(kCt)^{1/2} \quad (4)$$

From the slope of the $I_{\text{catal}}/I_{\text{d}}$ vs. $t^{1/2}$ plot (Fig. 6D), the value of k for 350 μM hydrazine was calculated to be 2.22×10^5 cm^3 mol^{-1} s^{-1}.

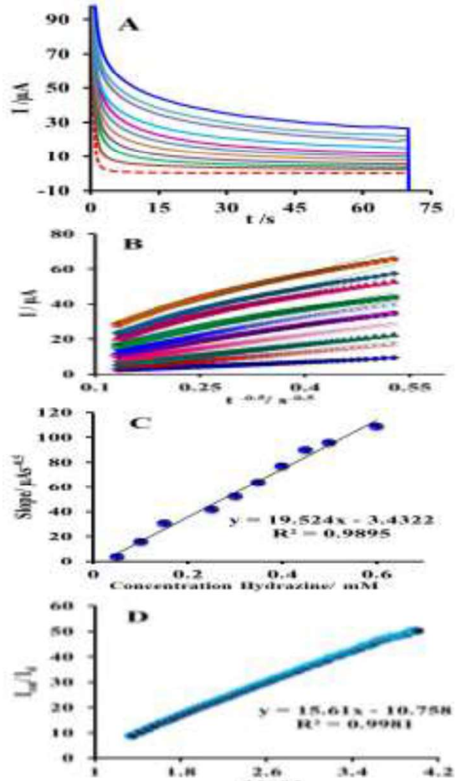

Fig. 6. (A) Chronoamperograms of CuNPs/P-Gly/GONs/GCE in 0.1 M PBS (pH 7.0) containing different concentrations of hydrazine; chronoamperograms correspond to 0.0, 50.0, 100.0, 150.0, 200.0, 250.0, 300.0, 350.0, 400.0, 500.0 and 600.0 μM of hydrazine (from bottom to top). (B) Plot of I versus $t^{-1/2}$ from the data of chronoamperograms for different concentrations of hydrazine. (C) The slopes of resulting straight lines from (B) versus hydrazine concentration. (D) Dependency of $I_{\text{catal}}/I_{\text{d}}$ on $t^{1/2}$ derived from CAs of a and e in panel A; potential step = 0.266 V.

3.7. Selectivity and stability of modified electrode sensor

The effect of electroactive interfering species on the modified electrode was evaluated. Fig. 7, shows the amperometric response of the Cu-NPs/p-Gly/GONs/GCE towards the successive addition of hydrogen peroxide, glucose, oxalic acid, PO_4^{2-}, Na^+, K^+, Mg^{2+}, Ba^{2+}, SO_4^{2-}, CH_3COO^-, Cl^- in 0.1 M PBS solution (pH 7.0) at 0.266 V. The results showed that these common interferences with the added concentration (1000 times to hydrazine concentration) did not affect the determination of hydrazine. In addition, the amperometric responses to 20 µM hydrazine were almost constant both before and after these solutions were added, indicating the high anti-interference ability of the presented sensor. One of the advantages of the modified electrode for amperometric detection of hydrazine is its highly stable amperometric response during a long period towards hydrazine oxidation. The amperometric response of 20 µM hydrazine was recorded over 50 min periods (data not shown). The response remained stable throughout the experiment, indicating that the Cu-NPs/p-Gly/GONs/GCE imparted higher stability for amperometric measurements of hydrazine.

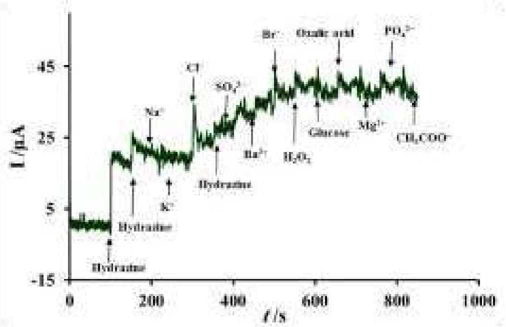

Fig. 7. amperometric *i–t* response at CuNPs/P-Gly/GONs/GCE hydrazine and interference of hydrogen peroxide, glucose, oxalic acid, PO_4^2, Na^+, K^+, Mg^{2+}, Ba^{2+}, SO_4^{2-}, CH_3COO^-, Cl^-.

4. CONCLUSION

We developed a novel sensor for the analytical detection of hydrazine based on the incorporation of Cu-NPs onto the p-Gly/GONs/GCE nanocomposite film. The modified electrode exhibited high sensitivity and selectivity to hydrazine by significantly enhancing the oxidation peak current and the effect of other interfering compounds was completely eliminated. Moreover, a remarkable improvement in the kinetics of the electron transfer for hydrazine was observed on the surface of the Cu-NPs/p-Gly/GONs modified electrode, by lowering the anodic overpotential and considerably increasing the anodic peak current. The advantages of the proposed sensor are low cost, easy to fabricate, highly stable, very sensitive, specific response to hydrazine, and more convenient as compared with other reports sensors.

ACKNOWLEDGEMENTS

The authors gratefully acknowledge the Research Council of Payame Noor University for its financial support.

REFERENCES

[1] K.S. Novoselov, A.K. Geim, S.V. Morozov, D. Jiang, Y. Zhang, S.V. Dubonos, I.V . Grigorieva and A.A. Firsov, Electric field effect in atomically thin carbon films, *Science*, 306 (2004) 666–669.

[2] S. Stankovich, D.A .Dikin, G.H.B. Dommett, K.M . Kohlhaas, E.J. Zimney, E.A . Stach, R.D. Piner, S.T.Nguyen, R.S. Ruoff, Graphene based-composite materials, *Nature*, 442 (2006) 282–286.

[3] J.S. Bunch, A.M. van der Zande, S.S. Verbridge, I.W. Frank, D.M. Tanenbaum, J.M. Parpia, H.G .Craighead ,P.L .McEuen, Electromechanical resonators from graphene sheets ,*Science*, 315 (2007) 490–493.

[4] H. Deng, M. Zhu, T. Jin, C. Cheng, J. Zheng, Y. Qian, One-step synthesis of nitrogen, sulphur-codoped graphene as electrode material for supercapacitor with excellent cycling stability, *Int. J. Electrochem. Sci*. 15 (2020) 16–25.

[5] J. Liu, C.K. Poh, D. Zhan, L. Lai, S.H. Lim, L. Wang, X. Liu, N.G. Sahoo, C. Li, Z. Shen, Improved synthesis of grapheneflakes from the multiple electrochemical exfoliation of graphite rod, *Nano Eng*. 2 (3) (2013) 377–386.

[6] X. Fan, Y. Xu, T. Sheng, D. Zhao, H. Yuan, F. Liu, X. Liu, X. Zhu, L. Zhang, J. Lu, Amperometric sensor for dopamine based on surface-graphenization pencil graphite electrode prepared by in-situ electrochemical delamination, *Microchim. Acta* 186 (5) (2019) 324.

[7] C.-H. Chen, S.-W. Yang, M.-C. Chuang, W.-Y. Woon, C.-Y. Su, Towards the continuous production of high crystallinity graphene via electrochemical exfoliation with molecular in situ encapsulation, *Nanoscale* 7 (37) (2015) 15362–15373.

[8] Y. Vasseghian, D. Elena-Niculina, M. Moradi, and A. Mousavi Khaneghah. A review on graphene-based electrochemical sensor for mycotoxins detection, *Food and Chemical Toxicology* 148 (2021) 111931.

[9] S. Gupta, C. N. Murthy, and C. R. Prabha. Recent advances in carbon nanotube based electrochemical biosensors. International journal of biological macromolecules 108 (2018) 687-703.

[10] H. Song, Z. Xiaoyuan, L. Yunfang, and S. Zhiqiang. Developing Graphene‐Based Nanohybrids for Electrochemical Sensing, *The Chemical Record* 19 (2019) 534-549.

[11] R. Lakra, R. Kumar, P. K. Sahoo, D. Thatoi, and A. Soam. A mini-review: Graphene based composites for supercapacitor application, *Inorganic Chemistry Communications* 133 (2021) 108929.

[12] K.I. Bolotin, K.J. Sikes, Z. Jiang, M. Klima, G. Fudenberg, J. Hone, P. Kim, H.L. Stormer, Ultrahigh electron mobility in suspended graphene, *Solid State munications*, 146 (2008) 351–355.

[13] A.A. Balandin, S. Ghosh, W. Bao, I. Calizo, D. Teweldebrhan, F. Miao, C.N. Lau, Superior thermal conductivity of single-layer graphene, *Nano Letters*, 8(2008) 902–907.

[14] H. Beitollai, S. Mohadeseh, and S. Tajik. "Application of Graphene and Graphene Oxide for modification of electrochemical sensors and biosensors: A review." *Int. J. Nano Dim.* 10, no. 2 (2019): 125-140.

[15] H. Kumar, N. Venkatesh, H. Bhowmik, & A. Kuila, Metallic nanoparticle: a review. *Biomed. J. Sci. & Tech. Rese.* 4(2) (2018) 3765-3775.

[16] Y. Wu, Z. Jianhua, and H. Lu, A review of three-dimensional graphene-based materials: Synthesis and applications to energy conversion/storage and environment, *Carbon* 143 (2019) 610-640.

[17] W. Zhao, W. Zhenhui, Q. Li, Fabrication of a nichrome electrode coated with silver microcrystals, and its application to sensing hydrogen peroxide, *Anal. Methods*, 4(2012) 1105-1109.

[18] F.C. Pereira, M.V.B. Zanoni, Voltammetric sensor for sodium nitroprusside determination in biological fluids using films of poly-L-lysine, *Electroanalysis*, 19 (2007)993– 998.

[19] J.-B. Raoof, R. Ojani, and S. Rashid-Nadimi, Preparation of polypyrrole/ferrocyanide films modified carbon paste electrode and its application on the electrocatalytic determination of ascorbic acid, Electrochim. Acta., 49(2004) 271–280.

[20] Y Huang, F Bao, M Ji, Y Hu, L Huang, H Liu, J. Yu, G. Cong, C. Zhu, and J. Xu. A polyaniline-modified electrode surface for boosting the electrocatalysis towards the hydrogen evolution reaction and ethanol oxidation reaction, *Chem. Commun* .57, no. 100 (2021) 13792-13795.

[21] J.V. de Melo, M.E. Bello, W.M. de Azevêdo, J.M. de Souza, F.B. Diniz, The effect of glutaraldehyde on the electrochemical behavior of polyaniline, *Electrochim. Acta.*, 44 (1999) 2405–2412.

[22] E. Zhang, Z. Wang, Y. Zhang, Z. Zheng, C. Wang, Y. Du, W. Ye, Simultaneous electrochemical determination of uric acid, xanthine and hypoxanthine based on poly(l-arginine)/graphene composite film modified electrode, *Talanta*, 93 (2012) 320–325.

[23] X. Liu, L. Luo, Y. Ding, D. Ye, Poly-glutamic acid modified carbon nanotube-doped carbon paste electrode for sensitive detection of L-tryptophan, *Bioelectrochemistry*, 82 (2011) 38–45.

[24] E. Saeb, K. Asadpour-Zeynali, Facile synthesis of TiO_2@ PANI@ Au nanocomposite as an electrochemical sensor for determination of hydrazine, *Microchem. J.* 160 (2021) 105603.

[25] H. Wang, J. Ding, P. Kannan, S. Ji, Cobalt nanoparticles intercalated nitrogen-doped mesoporous carbon nanosheet network as potential catalyst for electro-oxidation of hydrazine, *Int. J. Hydrog. Energy*. 45 (38) (2020) 19344-19356.

[26] W.S. Hummers Jr, R.E. Offeman, Preparation of graphitic oxide, *J. Am. Chem. Soc.*, 80 (1958) 1339–1339.

[27] A.J. Bard, L.R. Faulkner, *Electrochemical Methods, Fundamentals and Applications*, Wiley, New York, 1980.

[28] Q. Chong, Z. Mei, L. Shanshan, G. Xinlei, W. Wei, H. Guanghui, Determination of hydrazine in prednisolone by derivatization-gas chromatography-triple quadrupole mass spectrometry, *Chin. J. Chromatogr*. 39 (7) (2021) 750.

[29] B. Habibi, S. Pashazadeh, L.A. Saghatforoush and A. Pashazadeh. "Direct electrochemical synthesis of the copper based metal-organic framework on/in the heteroatoms doped graphene/pencil graphite electrode: Highly sensitive and selective electrochemical sensor for sertraline hydrochloride." *J. Electroanal. Chem.* 888 (2021) 115210-115222.

[30] B. Habibi, S. Pashazadeh, L. A. Saghatforoush, and A. Pashazadeh, A thioridazine hydrochloride electrochemical sensor based on zeolitic imidazolate framework-67-functionalized bio-mobile crystalline material-41 carbon quantum dots. *New J. Chem*. 45 (32) (2021) 14739-50.

[31] G. Karim-Nezhad, R. Jafarloo, P. Seyed Dorraji, Copper (hydr) oxide modified copper electrode for electrocatalytic oxidation of hydrazine in alkaline media, *Electrochim.* Acta., 54 (2009) 5721– 5726.

[32] C.D.D.C. Conceicao, R.C. Faria, O. Fatibello-Filho, A.A. Tanaka, Electrocatalytic oxidation

and voltammetric determination of hydrazine in industrial boiler feed water using a cobalt phthalocyanine-modified electrode, *Anal. Lett.* 41 (2008) 1010–1021.

[33] M.R. Majidi, A. Jouyban, K. Asadpour-Zeynali, Electrocatalytic oxidation of hydrazine at overoxidized polypyrrole film modified glassy carbon electrode, *J. electrochim. Acta*., 52 (2007) 6248–6253.

[34] A. Abbaspour, A. Khajehzadeh, A. Ghaffarinejad, Electrocatalytic oxidation and determination of hydrazine on nickel hexacyanoferrate nanoparticles-modified carbon ceramic electrode, *J. Electroanal.Chem.*, 631 (2009) 52–57.

[35] N. Nasirizadeh, H.R. Zare, A.R. Fakhari, H. Ahmar, M.R. Ahmadzadeh, A. Naeimi, A study of the electrochemical behavior of an oxadiazole derivative electrodeposited on multi-wall carbon nanotube-modified electrode and its application as a hydrazine sensor, *J. Solid State Electrochem*., 15 (2011) 2683–2693.

[36] H. Zhang, J. Huang, H. Hou, T. You, Electrochemical detection of hydrazine based on electrospun palladium nanoparticle/carbon nanofibers, *Electroanalysis*, 21 (2009) 1869–1874.

[37] X. Ji, C.E. Banks, A.F. Holloway, K. Jurkschat, C.A. Thorogood, G.G. Wildgoose, R.G. Compton, Palladium Sub-Nanoparticle Decorated ‘Bamboo’ Multi-Walled Carbon Nanotubes Exhibit Electrochemical Metastability: Voltammetric Sensing in Otherwise Inaccessible pH Ranges, *Electroanalysis*, 18 (2006) 2481–2485.

[38] A.A. Ensafi, E. Mirmomtaz, Electrocatalytic oxidation of hydrazine with pyrogallol red as a mediator on glassy carbon electrode, *J. Electroanal.Chem.*, 583 (2005) 176–183.

[39] H. Ahmar, S. Keshipour, H. Hosseini, A.R. Fakhari, A. Shaabani, A. Bagheri, Electrocatalytic oxidation of hydrazine at glassy carbon electrode modified with ethylenediamine cellulose immobilized palladium nanoparticles, *J. Electroanal. Chem*., 690(2013) 96–103.

[40] G. Karim-Nezhad, L. Samandari, Thiourea Modified Copper Electrode: Application to Electrocatalytic Oxidation of Hydrazine, Anal. Bioanal. *Electrochem*, 6 (2014) 545-558.

[41] Q. Yi and W. g. Yu, Nanoporous gold particles modified titanium electrode for hydrazine oxidation, *J. Electroanal. Chem*., 633 (2009) 159–164.

[42] D. Afzali, H.K. Maleh, M.A. Khalilzadeh, Sensitive and selective determination of phenylhydrazine in the presence of hydrazine at a ferrocene-modified carbon nanotube paste electrode, *Environ. Chem. Lett*., 9 (2011) 375–381.

[43] G. Rani, M. Kumar, Amperometric Determination of Hydrazine Based on Copper Oxide Modified Screen Printed Electrode, *Sensors & Transducers*. 223 (7) (2018) 22-25.

[44] L. Ning, X. Guan, J. Ma, M. Wang, X. Fan, G. Zhang, F. Zhang, W. Peng, Y. Li, A highly sensitive nonenzymatic H_2O_2 sensor based on platinum, $ZnFe_2O_4$ functionalized reduced graphene oxide, *J. Alloys Compd*. 738 (2018) 317-322.

[45] T. Zhou, P. Lu, Z. Zhang, Q. Wang, A. Umar, Perforated Co3O4 nanoneedles assembled in chrysanthemum-like Co3O4 structures for ultra-high sensitive hydrazine chemical sensor, *Sens. Actuators B Chem*. 235 (2016) 457-465.

مطالعه رفتار الکتروشیمیایی هیدرازین در سطح الکترود کربن شیشه ای اصلاح شده با لایه های نازک پلیمری دوپه شده با نانوذرات مس

قاسم کریم نژاد[*۱]، **سارا پاشازاده**[۲]، **سمیرا هنرمند**[۱]

۱. گروه شیمی، دانشگاه پیام نور، صندوق پستی ۴۶۹۷- ۱۹۳۹۵، تهران، ایران

[۲] گروه شیمی، دانشکده علوم، دانشگاه شهید مدنی آذربایجان، تبریز ۵۳۷۱۴-۱۶۱، ایران

تاریخ دریافت: ٤ مرداد ۱٤۰۰ تاریخ پذیرش: ۱۸ شهریور ۱٤۰۰

چکیده

در این مطالعه، یک حسگر الکتروشیمیایی جدید با استفاده از نانو ورقه‌های گرافن اکسید ، الکتروپلیمریزاسیون پلی گلیسین و سنتز در محل فیلم نانوذرات مس تهیه شد. این سنسور برای بررسی رفتار الکتروشیمیایی هیدرازین استفاده شد. از میکروسکوپ الکترونی روبشی و طیف سنجی پراش اشعه ایکس برای بیان ویژگی های فیلم تهیه شده استفاده شد. در مقایسه با الکترود اصلاح نشده، پتانسیل پیک آندی اکسیداسیون هیدرازین در سطح الکترود اصلاح شده حدود ۱۵۰ میلی ولت به سمت مقادیر منفی جابجا می شود. پارامترهای سینتیکی از قبیل ضریب انتقال الکترون (α) و ثابت سرعت انتقال بار (k) برای اکسیداسیون هیدرازین با استفاده از ولتامتری چرخه ای تعیین شد. ضریب انتشار (D) هیدرازین نیز با استفاده از روش کرونوآمپرومتری محاسبه شد. محدوده تشخیص دینامیکی این حسگر نسبت به هیدرازین در سطح الکترود اصلاح شده با استفاده از روش آمپرومتری در محدوده ۶۰-۵ و ۱۵۰-۸۰ میکرومولار می باشد و حد تشخیص روش حدود ۵/۳۳ میکرومولار به دست آمد. یک روش ولتامتری جدید برای اندازه گیری هیدرازین ایجاد شد که حساسیت و گزینش پذیری خوب و محدوده خطی گسترده تری را نشان می دهد.

واژه‌های کلیدی

هیدرازین؛ الکترود کربن شیشه ای اصلاح شده؛ نانو ذره مس؛ گلیسین؛ نانو ورقه های گرافن اکسید.